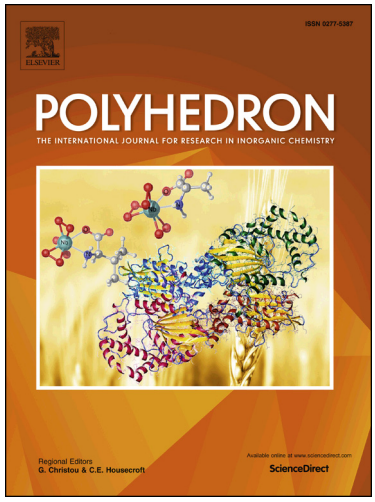

Synthesis, characterization and antimicrobial activity of novel 3-ferrocenyl-2-pyrazolyl-1,3-thiazolidin-4-ones

Anka Pejović, Aleksandra Minić, Jovana Bugarinović, Marko Pešić, Ivan Damljanović, Dragana Stevanović, Vladimir Mihailović, Jelena Katanić, Goran A. Bogdanović

PII: S0277-5387(18)30539-4
DOI: https://doi.org/10.1016/j.poly.2018.08.071
Reference: POLY 13394

To appear in: *Polyhedron*

Received Date: 12 July 2018
Accepted Date: 27 August 2018

Please cite this article as: A. Pejović, A. Minić, J. Bugarinović, M. Pešić, I. Damljanović, D. Stevanović, V. Mihailović, J. Katanić, G.A. Bogdanović, Synthesis, characterization and antimicrobial activity of novel 3-ferrocenyl-2-pyrazolyl-1,3-thiazolidin-4-ones, *Polyhedron* (2018), doi: https://doi.org/10.1016/j.poly.2018.08.071

Synthesis, characterization and antimicrobial activity of novel 3-ferrocenyl-2-pyrazolyl-1,3-thiazolidin-4-ones

Anka Pejović,*[a] Aleksandra Minić,[a] Jovana Bugarinović,[a] Marko Pešić,[a] Ivan Damljanović,[a] Dragana Stevanović,[a] Vladimir Mihailović,[a] Jelena Katanić[a] and Goran A. Bogdanović[b]

[a]*Department of Chemistry, Faculty of Science, University of Kragujevac, R. Domanovića 12, 34000 Kragujevac, Serbia*

[b]*Vinča Institute of Nuclear Sciences, University of Belgrade, PO Box 522, 11001 Belgrade, Serbia*

E-mail address: apejovic@kg.ac.rs (A. Pejović)

Abstract: A new series of ferrocene-containing thiazolylpyrazoles – 3-ferrocenyl-2-pyrazolyl-1,3-thiazolidin-4-ones have been synthesized using convenient one-pot three component condensation. Twelve newly synthesized compounds were fully characterized by spectroscopic (IR and NMR) and electrochemical methods (cyclic voltammetry). Single crystal X-ray structure analysis were undertaken on two compounds. The twelve novel ferrocene derivatives were also evaluated for antimicrobial activity. The results showed moderate antimicrobial activity of synthesized compounds with better effect on *Candida albicans* and Gram-negative bacteria than Gram-positive bacterial strains.

Keywords: Ferrocene, 1,3-Thiazolidin-4-one, Pyrazole, Crystal structure, Electrochemistry, Antimicrobial activity

∗ Corresponding author. e-mail: anka.pejovic@gmail.com

1. Introduction

Since the middle of the 20th century, the antimicrobial agents have been efficiently used in health care. However, in the recent time the success in the application of antibiotics in treating of infections has been eroded by the increased resistance of bacteria. Therefore, there is a permanent interest in the development of novel substances exhibiting antimicrobial activity [1, 2]. Certain organometallic compounds offer a promise in this respect, because they are inert, often uncharged, and fairly lipophilic [3]. The metal centers exist in low oxidation states, which limit the danger of oxidative damage inside cells [3]. It was found that ferrocene and some of its derivatives (e.g., ferrocifen) have strong and useful pharmacological properties and are considered as promising lead structures,particularly it is found that ferrocene itself have some antiproliferative activity. Its mechanism of action remains elusive despite several efforts; however, it is assumed by some researchers that the redox chemistry (Fe^{2+}/Fe^{3+}) is the core of its activity [3].

On the other side, the sulfur and nitrogen fused heterocycles in their own are very interesting due to their physicochemical properties, especially in the sense of designing new drugs and new materials. The chemistry and pharmacology of thiazolidinone derivatives has been of great interest to medicinal chemists lately [4–9]. The pyrazole ring is a prominent structural moiety found in numerous pharmacologically active compounds. Pyrazole-based derivatives have been regarded as anxiolytics [10], γ-gaminobutyric acid (GABA) receptor antagonists and insecticides [11], potential positron emission tomography (PET) ligands for cannabinoid receptors type 1 (CB1) [12], anti-inflammatory, antimicrobial [13], and growth inhibition agents [14].

Several years ago, we described the efficient synthetic route to the 3-ferrocenyl-1-phenylpyrazole-4-carboxaldehyde **3** (Scheme 1) [15]. Moreover, we discovered that this class of compound represents an excellent starting material for the synthesis of a numerous novel ferrocene-containing products [15]. In continuation of our ongoing interest in synthesis of ferrocene-containing heterocyclic compounds of potential biological interest [16–19], and having in mind the above considered, we have been prompted to synthesize new, possible more potent, pharmacologically active compounds. We decided to evaluate the potential application of the compound **3** (Scheme 1) in the synthesis of novel ferrocene-containing thiazolylpyrazoles – via one–pot three–component condensation, expecting (based on their structure) that the resulting novel ferrocene-containing heterocycles would be biologically active. Therefore, in the present paper we aim to report the design and synthesis of the

3-ferrocenyl-2-pyrazolyl-1,3-thiazolidin-4-ones. Furthermore, the results of antibacterial and antifungal examinations of all newly synthesized compounds are presented, as well as the results of electrochemical investigations and X-ray analyses.

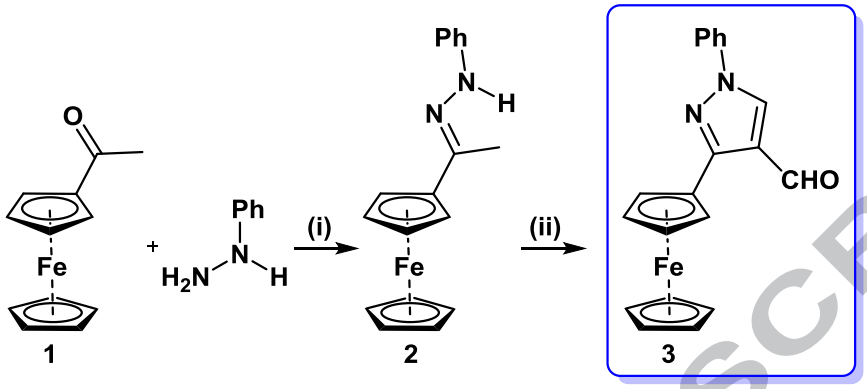

Scheme 1. Synthesis of 3-ferrocenyl-1-phenylpyrazole-4-carboxaldehyde **3** [15]; (i) Ethanol, reflux; (ii) $POCl_3$ (3 equiv), DMF, r.t.;

2. Experimental Section

2.1 Materials and measurements

All chemicals were commercially available and used as received, except that the solvents were purified by distillation. Chromatographic separations were carried out using silica gel 60 (Merck, 230–400 mesh ASTM), whereas silica gel 60 on Al plates, layer thickness 0.2 mm (Merck) was used for TLC. Electrochemical measurements were performed at room temperature in a three-electrode cell using an Autolab potentiostat (PGSTAT 302N). The working electrode was a glassy carbon disk (2 mm diameter). The counter electrode was a platinum wire, and Ag/AgCl electrode was used as the reference electrode. Melting points (uncorrected) were determined on a Mel-Temp capillary melting points apparatus, model 1001. The ^{1}H and ^{13}C NMR spectra of the samples in $CDCl_3$ were recorded on a Bruker Avance III 200 MHz (^{1}H at 200 MHz, ^{13}C at 50 MHz) NMR spectrometer. Chemical shifts are expressed in δ (ppm), relative to residual solvent protons as the internal standard ($CDCl_3$: 7.26 ppm for ^{1}H and 77 ppm for ^{13}C). IR measurements were carried out with a Perkin–Elmer FTIR 31725-X spectrophotometer.

2.2. Synthetic procedures

2.2.1. Synthesis of 3-ferrocenyl-1-phenylpyrazole-4-carboxaldehyde 3

3-Ferrocenyl-1-phenylpyrazole-4-carboxaldehyde **3** was synthesized according to previously described procedure [15].

2.2.2 Synthesis of 2-(3-ferrocenyl-1-phenyl-1*H*-pyrazol-4-yl)thiazolidin-4-ones 5a–l

General procedure

An ice-cooled solution of the corresponding primary amine (1 mmol) and 3-ferrocenyl-1-phenylpyrazole-4-carboxaldehyde **3** (356 mg, 1 mmol) in THF (2 mL) was irradiated in an ultrasonic bath for 5 min, followed by the addition of thioglycolic acid (184 mg, 2 mmol). After further irradiation for 5 min, DCC (206 mg, 1 mmol) was added to the resulting mixture and irradiation continued for another 15 min under the same conditions. DCU was removed by filtration, the solvent evaporated, and the residue taken up in EtOAc (30 mL). The organic layer was washed with 5% aq. solution of citric acid, H_2O, 5% aq. solution of $NaHCO_3$ and brine, successively, and dried overnight (anh. Na_2SO_4). After the evaporation of the solvent, the crude mixture was purified by column chromatography (SiO_2/hexane – EtOAc 7:3, v/v).

2-(3-Ferrocenyl-1-phenyl-1-*H*-pyrazol-4-yl)-3-methylthiazolidin-4-one (**5a**). Orange solid. Yield (91 %), m.p. 136 °C; IR (KBr): ν = 3093, 2923, 1683, 1599, 1553, 1506 cm^{-1}; ^1H NMR (200 MHz, $CDCl_3$, ppm): δ 7.85 (s, 1H), 7.77 – 7.61 (m, 2H), 7.53 – 7.38 (m, 2H), 7.37 – 7.23 (m, 1H), 6.02 (s, 1H), 4.29 (s, 5H), 4.97 – 3.95 (m, 4H), 3.90 – 3.54 (m, 2H), 2.91 (s, 3H); ^{13}C NMR (50 MHz, $CDCl_3$, ppm): δ 170.9, 170.7, 149.6, 139.4, 129.3, 126.5, 125.9, 120.2, 118.7, 70.3, 69.8, 68.9, 67.9, 56.8, 32.9, 30.5.

3-Butyl-2-(3-ferrocenyl-1-phenyl-1-*H*-pyrazol-4-yl)thiazolidin-4-one (**5b**). Orange solid. Yield (71 %), m.p. 133 °C; IR (KBr): ν = 3126, 2927, 1674, 1598, 1555, 1506 cm^{-1}; ^1H NMR (200 MHz, $CDCl_3$, ppm): δ 7.79 (s, 1H), 7.75 – 7.56 (m, 2H), 7.54 – 7.36 (m, 2H), 7.34 – 7.20 (m, 1H), 6.02 (s, 1H), 4.98 – 4.06 (m, 4H), 4.27 (s, 5H), 3.89 – 3.55 (m, 3H), 3.06 – 2.70 (m, 1H), 1.64 – 1.14 (m, 4H), 0.87 (t, J = 6.4 Hz, 3H); ^{13}C NMR (50 MHz, $CDCl_3$, ppm): δ 170.8, 149.4, 139.6, 129.4, 126.5, 125.6, 121.0, 118.7, 70.4, 69.8, 69.1, 67.8, 55.2, 43.2, 32.8, 29.4, 20.1, 13.8.

2-(3-Ferrocenyl-1-phenyl-1-*H*-pyrazol-4-yl)-3-hexylthiazolidin-4-one (**5c**). Dark red solid. Yield (69 %), IR (KBr): ν = 3090, 2926, 1676, 1599, 1552, 1505 cm^{-1}; ^1H NMR (200 MHz, $CDCl_3$, ppm): δ 7.81 (s, 1H), 7.77 – 7.70 (m, 2H), 7.54 – 7.40 (m, 2H), 7.36 – 7.24 (m, 1H), 6.02 (s, 1H), 4.74– 4.60 (m, 2H), 4.43 – 4.32 (m, 2H), 4.19 (s, 5H), 3.87 – 3.60 (m, 3H), 2.88 (dt, J = 13.8, 6.8 Hz, 1H), 1.61 – 1.38 (m, 2H), 1.36 – 1.10 (m, 6H), 0.82 (t, J = 6.1 Hz, 3H).; ^{13}C NMR (50 MHz, $CDCl_3$, ppm): δ 170.8, 149.4, 139.6, 129.4, 126.5, 125.5, 121.0, 118.7, 69.6, 68.9, 68.5, 67.1, 55.1, 43.3, 32.6, 31.3, 27.2, 26.5, 22.5, 13.9.

2-(3-Ferrocenyl-1-phenyl-1-*H*-pyrazol-4-yl)-3-octylthiazolidin-4-one (**5d**). Orange solid. Yield (60 %); IR (KBr): ν = 3123, 2925, 1676, 1599, 1555, 1506 cm^{-1}; ^1H NMR (200 MHz, $CDCl_3$, ppm): δ 7.79 (s, 1H), 7.74 – 7.60 (m, 2H), 7.53 – 7.38 (m, 2H), 7.36 – 7.25 (m, 1H), 6.01 (s, 1H), 5.03 – 4.05 (m, 4H), 4.29 (s, 5H), 3.87 – 3.51 (m, 3H), 3.05 – 2.67 (m, 1H), 1.67 – 1.38 (m, 2H), 1.38 – 1.03 (m, 10H), 0.84 (t, J = 5.9 Hz, 3H); ^{13}C NMR (50 MHz, $CDCl_3$, ppm): δ 170.7, 149.3, 139.4, 129.3, 126.4, 125.5, 120.9, 118.6, 70.4, 69.8, 69.1, 67.7, 55.1, 43.3, 32.7, 31.6, 29.1, 29.0, 27.2, 26.7, 22.5, 14.0.

3-Benzyl-2-(3-ferrocenyl-1-phenyl-1-*H*-pyrazol-4-yl)thiazolidin-4-one (**5e**). Orange solid. Yield (71 %); m.p. 169 °C; IR (KBr): ν = 3120, 2928, 1694, 1626, 1597, 1553, 1496 cm^{-1}; ^1H NMR (200 MHz, $CDCl_3$, ppm): δ 7.75 (s, 1H), 7.71 – 7.02 (m, 10H), 5.86 (s, 1H), 5.24 – 4.99 (m, 1H), 4.81 – 3.69 (m, 7H); 4.14 (s, 5H), ^{13}C NMR (50 MHz, $CDCl_3$, ppm): δ 171.1, 149.5, 139.4, 135.3, 129.3, 128.8, 127.8, 127.7, 126.4, 125.8, 120.1, 118.6, 70.3, 69.7, 68.8, 67.8, 54.8, 46.6, 32.7.

2-(3-Ferrocenyl-1-phenyl-1-*H*-pyrazol-4-yl)-3-(4-methoxyphenethyl)thiazolidin-4-one (**5f**). Dark red solid. Yield (83 %), IR (KBr): ν = 3081, 2927, 1674, 1599, 1552, 1512 cm^{-1}; ^1H NMR (200 MHz, $CDCl_3$, ppm): δ 7.72 (s, 1H), 7.71 – 7.60 (m, 2H), 7.54 – 7.36 (m, 2H), 7.34 – 7.21 (m, 1H), 7.02 (t, J = 8.4 Hz, 2H), 6.80 (t, J = 8.4 Hz, 2H), 5.78 (s, 1H), 4.82 – 4.64 (m, 1H), 4.50 – 4.31 (m, 3H), 4.19 (s, 5H), 3.99 – 3.68 (m, 3H), 3.74 (s, 3H), 3.19 – 2.92 (m, 1H), 2.89 – 2.65 (m, 2H); ^{13}C NMR (50 MHz, $CDCl_3$, ppm): δ 170.9, 158.3, 149.5, 139.5, 130.1, 129.6, 129.3, 126.5, 125.7, 120.7, 118.7, 114.0, 77.3, 69.9, 69.2, 69.1, 68.5, 67.4, 55.6, 55.2, 45.1, 32.7, 32.5.

2-(3-Ferrocenyl-1-phenyl-1-*H*-pyrazol-4-yl)-3-(furan-2-ylmethyl)thiazolidin-4-one (**5g**). Orange solid. Yield (64 %), m.p. 187 °C; IR (KBr): ν = 3080, 2914, 1691, 1599, 1557, 1506 cm^{-1}; ^1H NMR (200 MHz, $CDCl_3$, ppm): δ 7.89 – 7.56 (m, 3H), 7.55 – 7.20 (m, 4H), 6.31 – 6.23 (m, 1H), 6.22 – 6.14 (m, 1H), 6.01 (s, 1H), 5.16 – 3.98 (m, 6H), 4.24 (s, 5H), 3.97 – 3.56 (m, 2H); ^{13}C NMR (50 MHz, $CDCl_3$, ppm): δ 170.8, 149.5, 148.9, 142.4, 139.3, 129.3, 126.4, 125.8, 120.2, 118.6, 110.4, 108.9, 70.3, 69.6, 68.8, 67.8, 55.1, 39.7, 32.6.

2-(3-Ferrocenyl-1-phenyl-1-*H*-pyrazol-4-yl)-3-(thiophen-2-ylmethyl)thiazolidin-4-one (**5h**). Yellow solid. Yield (69 %), m.p. 180 °C; IR (KBr): ν = 3131, 2922, 1679, 1599, 1553, 1505 cm^{-1}; ^1H NMR (200 MHz, $CDCl_3$, ppm): δ 7.79 (s, 1H), 7.73 – 7.58 (m, 2H), 7.58 – 7.37 (m, 2H), 7.37 – 7.11 (m, 3H), 6.99 – 6.68 (m, 2H), 5.98 (s, 1H), 5.25 – 4.99 (m, 1H), 4.85 – 4.10 (m, 5H), 4.20 (s, 5H), 3.95 – 3.57 (m, 2H); ^{13}C NMR (50 MHz, $CDCl_3$, ppm): δ 170.8, 149.5, 139.3, 137.6, 129.3, 127.1, 126.8, 126.4, 126.0, 125.8, 119.9, 118.6, 70.2, 69.5, 68.7, 67.7, 54.6, 41.4, 32.6.

2-(3-Ferrocenyl-1-phenyl-1-*H*-pyrazol-4-yl)-3-(pyridin-2-ylmethyl)thiazolidin-4-one (**5i**). Orange solid. Yield (58 %), m.p. 172 °C; IR (KBr): ν = 3128, 2927, 1680, 1597, 1555, 1505 cm^{-1}; ^1H NMR (200 MHz, $CDCl_3$, ppm): δ 8.55 (s, 1H), 8.08 – 6.97 (m, 9H), 6.25 (s, 1H), 5.34 – 4.99 (m, 1H), 4.73 – 3.74 (m, 7H), 4.10 (s, 5H); ^{13}C NMR (50 MHz, $CDCl_3$, ppm): δ 171.5, 155.3, 149.6, 139.5, 136.9, 129.3, 126.4, 126.1, 122.6, 121.9, 120.1, 118.7, 70.1, 69.4, 68.5, 67.7, 55.6, 48.1, 32.6.

2-(3-Ferrocenyl-1-phenyl-1-*H*-pyrazol-4-yl)-3-(pyridin-3-ylmethyl)thiazolidin-4-one (**5j**). Yellow solid. Yield (75 %), m.p. 187 °C; IR (KBr): ν = 3127, 2934, 1689, 1597, 1553, 1497 cm^{-1}; ^{1}H NMR (200 MHz, $CDCl_3$, ppm): δ 9.57 (s, 1H), 8.05 – 7.00 (m, 9H), 5.88 (s, 1H), 5.27 – 4.87 (m, 1H), 4.75 – 4.59 (m, 1H), 4.41 – 4.04 (m, 4H), 4.10 (s, 5H), 3.92 – 3.67 (m, 2H); ^{13}C NMR (50 MHz, $CDCl_3$, ppm): δ 171.1, 149.6, 139.3, 129.3, 126.5, 119.7, 118.8, 69.5, 69.0, 68.8, 68.5, 67.3, 54.7, 32.6.

2-(3-Ferrocenyl-1-phenyl-1-*H*-pyrazol-4-yl)-3-*m*-tolylthiazolidin-4-one (**5k**). Orange solid. Yield (53 %); IR (KBr): ν = 3127, 2919, 1680, 1599, 1558, 1504 cm^{-1}; m.p. 167 °C; ^{1}H NMR (200 MHz, $CDCl_3$, ppm): δ 7.90 (s, 1H), 7.71 – 7.60 (m, 2H), 7.52 – 7.38 (m, 2H), 7.33 – 7.16 (m, 2H), 7.14 – 6.98 (m, 3H), 6.44 (s, 1H), 4.68 – 4.50 (m, 2H), 4.33 (t, J = 1.8 Hz, 2H), 4.11 (s, 5H), 4.00 – 3.83 (m, 2H), 2.28 (s, 3H); ^{13}C NMR (50 MHz, $CDCl_3$, ppm): δ 170.8, 149.0, 139.5, 139.2, 137.4, 129.3, 129.0, 128.1, 126.4, 125.9, 125.7, 122.6, 121.1, 118.6, 69.4, 68.8, 68.3, 67.3, 57.7, 33.2, 21.4.

2-(3-Ferrocenyl-1-phenyl-1-*H*-pyrazol-4-yl)-3-*p*-tolylthiazolidin-4-one (**5l**). Orange solid. Yield (34 %); IR (KBr): ν = 3115, 2921, 1683, 1599, 1555, 1503 cm^{-1}; ^{1}H NMR (200 MHz, $CDCl_3$, ppm): δ 7.92 (s, 1H), 7.77 – 6.95 (m, 9H), 6.44 (s, 1H), 4.67 – 4.50 (m, 2H), 4.41 – 4.26 (m, 2H), 4.23 – 3.78 (m, 2H), 4.12 (s, 5H), 2.27 (s, 3H); ^{13}C NMR (50 MHz, $CDCl_3$, ppm): δ 170.7, 149.0, 139.4, 137.1, 134.8, 129.8, 129.3, 126.3, 126.0, 125.4, 121.0, 118.6, 69.4, 68.8, 68.2, 67.3, 57.6, 33.4, 21.0.

2.3. X-ray data collection and structure refinement for compounds 5k and 5g

Single-crystal X-ray diffraction data for both compounds were collected on an Oxford Gemini S diffractometer equipped with a CCD detector, using monochromated Mo *K*α radiation. Data reduction and empirical absorption correction were performed with CrysAlisPRO [20]. Crystal structures were solved by direct methods using SHELXS and refined on F^2 by full-matrix least-squares using SHELXL [21]. All non-H atoms were refined anisotropically. All H atoms were placed in geometrically calculated positions and refined using the riding model with U_{iso} values constrained to $1.2U_{eq}$ or $1.5U_{eq}$ of the parent C atoms. Crystallographic details for structure analysis of the compounds **5k** and **5g** are summarized in Table 1. Figures were produced using MERCURY [22]. The software used for the preparation of the materials for publication: WINGX [23], PLATON [24], PARST [25].

Table 1. Crystallographic data and structure refinement for **5k** and **5g**.

Identification code	**5k**	**5g**
Empirical formula	C_{29} H_{25} Fe N_3 O S	C_{27} H_{23} Fe N_3 $O_{2.5}$ S
Formula weight	519.43	517.39
Color, crystal shape	Red, prism	Red, irregular
Crystal size (mm^3)	0.26 x 0.43 x 0.45	0.14 x 0.27 x 0.39
Temperature	298(2)	293(2)

Wavelength	0.71073	0.71073
Crystal system	Orthorhombic	Orthorhombic
Space group	*Pbca*	*Pbca*
Unit cell dimensions		
a (Å)	11.1233(2)	10.9102(5)
b (Å)	30.5974(6)	30.6164(11)
c (Å)	14.2239(2)	13.8706(5)
V (Å^3)	4841.02(15)	4633.2(3)
Z	8	8
D_{calc} (Mg/m^3)	1.425	1.483
μ (mm^{-1})	0.737	0.775
F(000)	2160	2144
θ range for data collection (°)	2.66-29.11	2.66-26.40
Index ranges	–12<=h<=14,	–13<=h<=13,
Reflections collected	28419	17406
Independent reflections, R_{int}	5781, 0.0242	4740, 0.0509
Completeness to θ = 26.00°	99.9 %	99.9 %
Data / restraints / parameters	5781 / 0 / 317	4740 / 0 / 316
Goodness-of-fit	1.072	1.077
Final R_1/wR_2 indices [$I > 2\sigma(I)$]	0.0460, 0.1082	0.0684, 0.1881
Final R_1/wR_2 indices (all data)	0.0563, 0.1140	0.0901, 0.2019
Largest diff. peak and hole (e.Å^{-3})	0.580, –0.577	0.359, –0.692

2.4. Antimicrobial activity determination

The ability of newly synthesized compounds to inhibit the growth of selected microorganisms was determined using microdilution method described by Sarker et al. [26], with some modifications described in our previous study [16].

The assays with tested compounds were performed on four bacterial ATCC cultures, two Gram-negative: *Salmonella enteritidis* ATCC 13076 and *Escherichia coli* ATCC 25922, two Gram-positive: *Enterococcus faecalis* ATCC 29212 and *Staphylococcus aureus* ATCC 25923; and one yeast *Candida albicans* ATCC 10231. All used microbial strains were obtained from the Institute of Public Health, Kragujevac, Serbia. The bacteria were cultivated on Nutrient agar at 37 °C for 24 h, while *C. albicans* was grown on Sabouraud dextrose agar at 28 °C for 48 h before the experiment.

All the assays for evaluation of antibacterial and antifungal activities were performed according to the NCCLS recommendations [27–29]. The growth of bacteria was monitored using the indicator resazurin and growth of *C. albicans* was monitored visually. Minimal inhibitory concentration (MIC) values, as the lowest concentration of compounds without visible bacterial or fungal growth, were expressed in mg per mL. Antibiotic Ciprofloxacin

was used as a positive control for evaluation of antibacterial activity, while Clotrimazole was a positive control for determination of antifungal potential.

3. Results and Discussion

3.1. Synthesis

One of the most prominent protocols for the 1,3-thiazolidin-4-ones synthesis is definitely the one–pot three–component condensation. This condensation occurs in the presence of a suitable dehydrating agent between amines, aldehydes and α-mercapto carboxylic acids [30–32]. Therefore, we considered to synthesize a series of novel ferrocene-containing 2-pyrazolyl-1,3-thiazolidin-4-ones and at the same time to evaluate the synthetic potential of 3-ferrocenyl-1-phenylpyrazole-4-carboxaldehyde **3** previously obtained in our laboratory [15]. Synthetic pathway for the preparation of 3-ferrocenyl-2-pyrazolyl-1,3-thiazolidin-4-ones **5a-l** included quite simple, elegant procedure, according to which mixture of primary amines, 3-ferrocenyl-1-phenylpyrazole-4-carboxaldehyde **3** [15]**,** α-mercapto carboxylic acids and dehydrating agent in the appropriate solvent was irritated in ultrasound bath at low temperature (around 0 ^{o}C). Therefore, the realization of this synthetic plan began with the preparation of the ferrocene containing 1-phenylpyrazole-4-carboxaldehyde **3** [see reference 15]. In the opening experiment, we performed the reaction by ultrasonic irradiation of the methylamine, aldehyde **3** and α-mercapto carboxylic acids in a 1:1:2 ratio, in the presence of *N*,*N*'-dicyclohexylcarbodiimide (DCC) using tetrahydrofuran as solvent. After the usual workup and column chromatography (SiO_2, n-hexane / EtOAc = 7:3, v/v), to our delight, the desired 1-phenylpyrazole-4-carboxaldehyde **5a** was obtained in an excellent yield (91%, Table 2, entry 1). This result was very satisfactory to us, so we accepted these reaction conditions as the optimal ones.

Table 2. Substrate scope of synthesis of 3-ferrocenyl-2-pyrazolyl-1,3-thiazolidin-4-ones **5a-l**

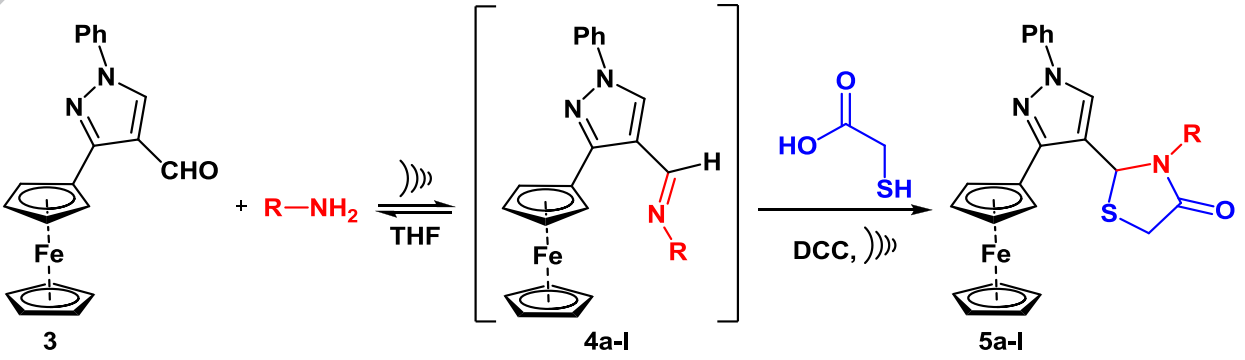

Entry	R	Product	Yields[a, b] (%)
1	Methyl	**5a**	91
2	n-Butyl	**5b**	71
3	n-Hexyl	**5c**	69
4	n-Octyl	**5d**	60
5	Benzyl	**5e**	71
6	2-(*p*-	**5f**	83
7	2-Furfuryl	**5g**	64
8	2-Thenyl	**5h**	69
9	2-Picolyl	**5i**	58
10	3-Picolyl	**5j**	75
11	m-Tolyl	**5k**	53
12	p-Tolyl	**5l**	34

[a]Isolated yield after column chromatography.
[b]Yields based on the starting 3-ferrocenyl-1-phenylpyrazole-4-carboxaldehyde **3**.

With the conditions in hand, we expanded our studies on eleven other primary amines (Table 2, Entries 2-12). All condensations were performed smoothly and the corresponding thiazolidinones **5a**–**l** were isolated pure in good to very high yields (see Table 2). As it is show the best results were achieved for the methyl and 4-methoxyphenethyl derivatives **5a** and **5f** (see Table 2, entry 1 (91%) and 6 (83%)), contrary to isolated *N*-aromatic compounds **5k** and **5l** which were obtained in yields of 53% and 34%, respectively (see Table 2, entry 11 and 12). Obtained results clearly indicate that structure of the starting primary amine has major influence on the reaction outcome.

In order to rationalize obtained results, we considered the reaction mechanism. The reaction of thiazolidinones formation has been the subject of study of the several research groups [33]. A proposed mechanism for the reaction is outlined in Scheme 2 *via* initial imine formation **4a-l** followed by attack of the sulfur moiety of the thioglycolic acid on the imine carbon to form the intermediate **A**. The next step involves intramolecular cyclization with the expulsion of water (caused by the presence of appropriate dehydrating agent - DCC) giving rise to the cyclized product thiazolidinone **5a-l**. Based on this mechanism, it is highly probable that lower yields obtained for the products **5k** and **5l** is caused by steric limitations of the staring substrate.

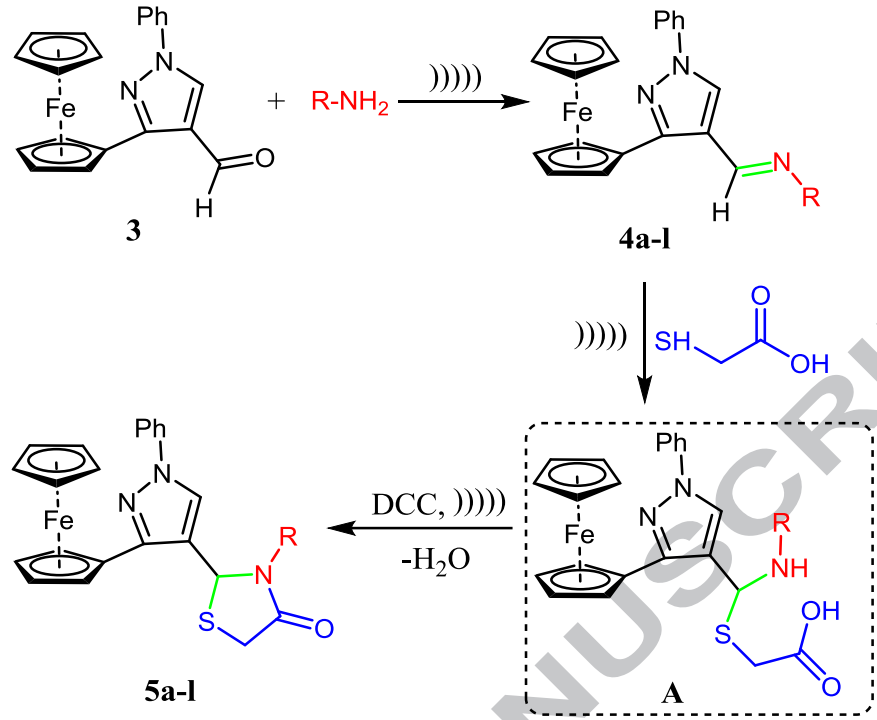

R the same as in the Table 2

Scheme 2. Plausible schematic mechanism for the synthesis of titled compound

3.2. Spectral characterization

All the synthesized thiazolidinones **5a–l** were characterized by the standard spectroscopic techniques (IR, and ^{1}H- and ^{13}C-NMR). The collected data were in complete agreement with the proposed structures.

The main common feature of the IR spectra of synthesized thiazolidinones **5a–l** is two strong bands at 1674–1694 cm^{-1} and 1557-1559 cm^{-1}, which are attributed to the C=O and C=N stretching, respectively. The ^{1}H NMR spectra of all twelve products contain signals of the cyclopentadienyl rings protons appear at the similar positions (δ = 4.19 ppm for the unsubstituted, and 3.69–5.16 ppm for substituted rings, respectively). Furthermore, in the ^{1}H NMR spectra of compounds **5a–l** characteristic signals for –N-CH$_2$, aromatic and aliphatic protons appear in the expected regions. In addition, in the ^{1}H NMR spectra of **5a–l**, one signal appears at about 6.02 ppm, origin of this signal corresponds to the methine protons of the thiazolidinone moiety. Further proof to confirm proposed structures for these compounds was provided by the X-ray crystal structure determinations of two representative thiazolidinones – **5k** and **5g**.

3.3. Crystal and molecular structures of 5k and 5g

Only **5k** and **5g** were obtained as single crystals suitable for X-ray diffraction studies. Both compounds crystallized in the same centrosymmetric space group *Pbca* with very similar unit cell dimensions. Their molecular structures are shown in Figures 1 and 2. In both molecules the Cp rings adopt nearly eclipsed geometry with the C1–Cg1–Cg2–C6 torsion angle of –2.3 and 0.9° for **5k** and **5g** respectively (Cg1 and Cg2 are centroids of the substituted and unsubstituted Cp rings).

The N1–N2–C11–C12–C13 five-membered ring is almost ideally planar in both molecules (root-mean-square deviations of the atoms which define the plane is 0.0012 and 0.0005 Å in **5k** and **5g** respectively). This heterocyclic ring is nearly coplanar with N1 bonded phenyl ring [Dihedral angle between two rings is 2.4(1) and 5.9(3)° in **5k** and **5g** respectively]. Dihedral angle between the N1 ring and the C1–C5 ciclopentadienyl ring is significantly different in two molecules [17.6(1) and 26.3(2)° for **5k** and **5g** respectively]. Another heterocyclic ring, the S1–C14–N3–C15–C16, adopts an envelope conformation with the S1 atom displaced from the mean plane defined by remaining four atoms for 0.619(3) and 0.566(8) Å in **5k** and **5g** respectively. The C14, N3, C15, C16 atoms which define the mean plane in the S1-ring are approximately coplanar (The torsion angle C14–N3–C15–C16 is 3.9(3) and 1.4 (6)° in **5k** and **5g** respectively).

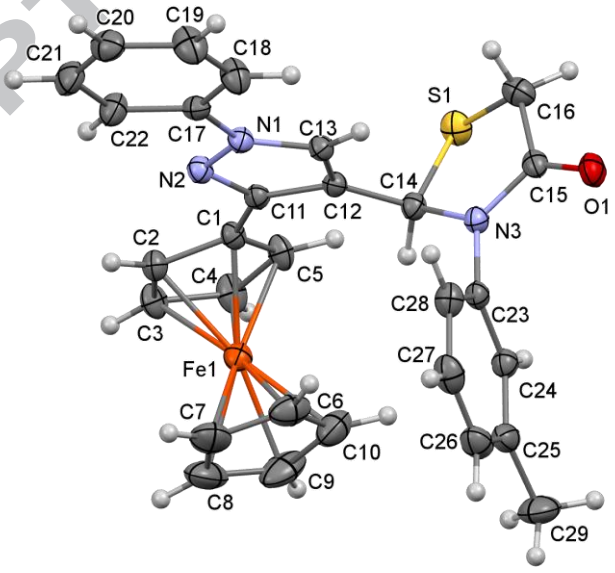

Figure 1. Molecular structure and numbering scheme of **5k** shown with atomic displacement parameters at the 30% probability level.

Corresponding bond distances in both compounds are very similar (Table 3). There are five N–C bonds in both molecules but only two of them (N3–C14 and N3–C23) are pure single bonds while the remaining three could be accepted as π delocalized bonds (Table 3). The S1 atom is bind to two sp^3 hybridized carbon atoms but the S1–C14 bond is somewhat longer than the S1–C16 (Table 3).

Although **5k** and **5g** do not contain any significant H-bond donor, both of them form compact centrosymmetric dimers with molecules interconnected by two C13–H…O1^{i} hydrogen bonds (Fig. 3). This H-bond in both crystal structures has similar geometrical parameters [H…O1^{i} distance 2.40 and 2.34 Å, C13–H…O1^{i} angle 156 and 167° in **5k** and **5g** respectively; symmetry code: (i) x+1/2,−y+1/2,−z+1]. In both structures the dimer has similar geometry (Fig. 3) and represents basic building unit in the crystal packing of two compounds. However there is another structural characteristic that is more interesting in the packing of both molecules: the formation of layers composed exclusively of ferrocene units. This is illustrated in two projections in Figures S1 and S2 (see in supplementary material). One can conclude that **5k** and **5g** regardless of significant dissimilarity in the N3-substituent, exhibit very similar structural properties in solid state as formation of dimers and accumulation of ferrocene units in separate sheets.

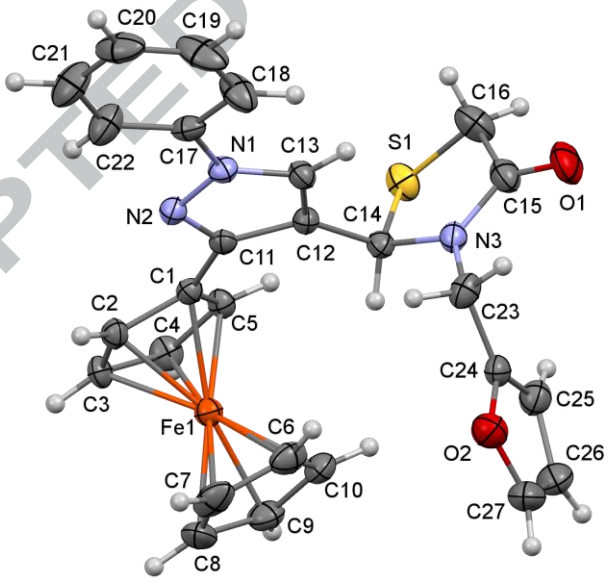

Figure 2. Molecular structure and numbering scheme of **5g** shown with atomic displacement parameters at the 30% probability level.

Table 3. Selected bond distances (Å) in crystal structures of **5k** and **5g**.

	5k	**5g**
S1–C16	1.799(3)	1.794(6)
S1–C14	1.839(2)	1.832(5)

O1–C15	1.217(3)	1.211(6)
N1–C13	1.355(3)	1.352(6)
N1–N2	1.364(2)	1.370(5)
N1–C17	1.419(3)	1.418(6)
N2–C11	1.330(3)	1.330(6)
N3–C15	1.354(3)	1.349(6)
N3–C23	1.432(3)	1.447(6)
N3–C14	1.467(2)	1.455(5)
C1–C11	1.462(3)	1.460(6)
C11–C12	1.422(3)	1.433(6)
C12–C13	1.373(3)	1.354(6)
C12–C14	1.492(3)	1.495(6)
C15–C16	1.511(3)	1.489(8)

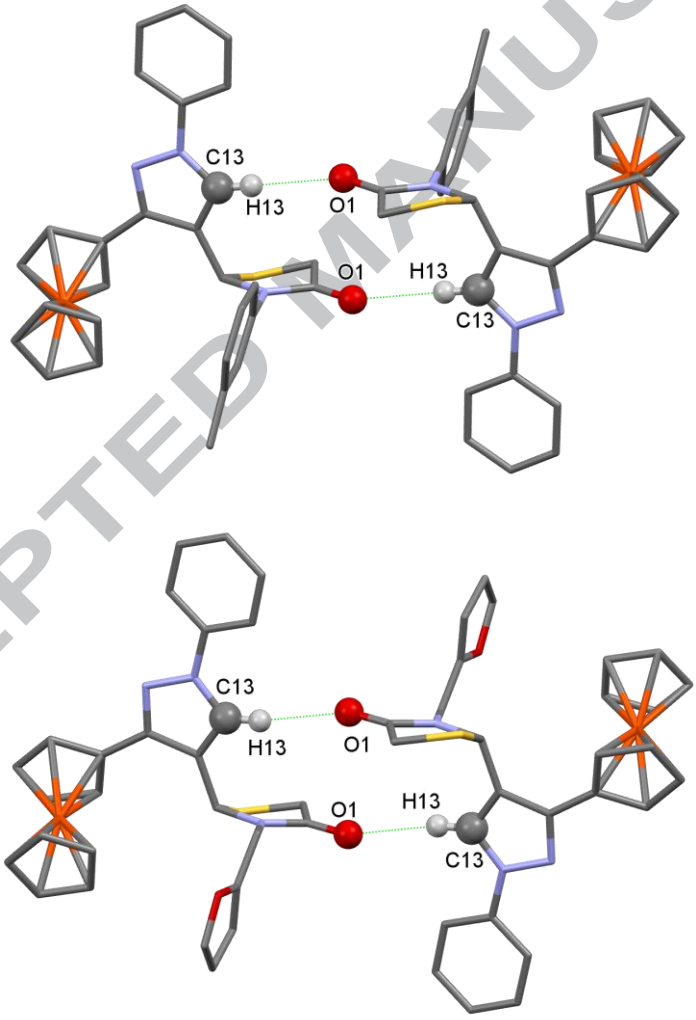

Figure 3. Centrosymmetric dimers of **5k** (top) and **5g** (bottom) formed in both crystal structures by means of the same C13–H…O1 hydrogen bond. H atoms (which are not involved in the formation of dimers) are omitted for clarity.

3.4. Electrochemistry

It is well known that the $Fe^{2+/}Fe^{3+}$ redox chemistry contributes to the bioactivity of ferrocene derivatives [34]. Leaded by this fact, we decided to evaluate the electrochemical properties of all the new compounds **5a–l**. This was done by the means of cyclic voltammetry in dichloromethane containing 0.1 mol/L tetrabutylammonium perchlorate as a supporting electrolyte. As a representative example we choose compound **5a** and the voltammograms (collected on deferent scan rate) are presented on the Figure 4, whereas the data obtained for all the other products are listed in the Table 4. As it has been shown in the Figure 4 (see curves **a)** the 2-(3-ferrocenyl-1-phenyl-1-*H*-pyrazol-4-yl)-3-methylthiazolidin-4-one **5a** exhibit reversible one–electron redox couple. Oxidation wave (O1) appear at 0.684 V, whereas the reduction one (R1) at 0.528 V, and we attributed them to the oxidation of ferrocene unit by the forward potential sweep, and the reduction of the obtained ferricinium ion at the back-potential sweep. These potentials are considerably more positive than the one of the unsubstituted ferrocene, as a consequence of the presence of heterocyclic group. The difference between those anodic and cathodic peak potentials (Table 4) is close to the theoretical value and independent of the scan rate v. Both, the anodic (O1) and cathodic (R1) peak currents are proportional to the square root of the scan rate, and their ratio is independent of the scan rate, indicating a diffusion-controlled (Figure 5), also the ratio of

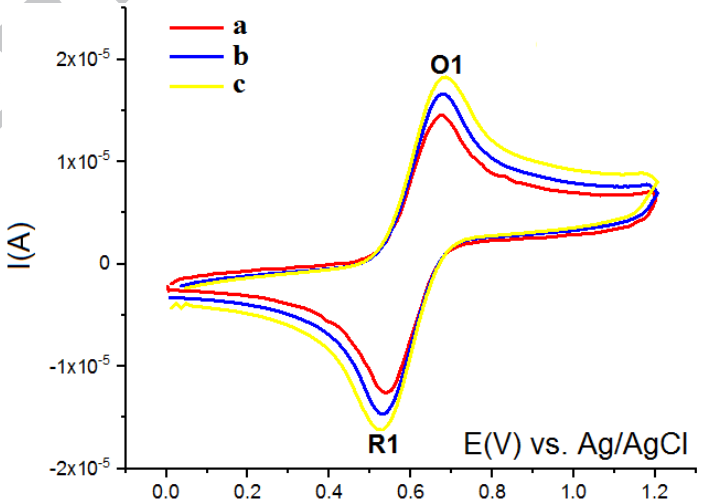

Figure 4. Cyclic voltammograms of 1 mM solution of 2-(3-Ferrocenyl-1-phenyl-1-*H*-pyrazol-4-yl)-3-methylthiazolidin-4-one (**5a**) at the glassy carbon electrode by a 0.1 V s^{-1} scan rate in 0.1 M dichloromethane solution of Bu_4NClO_4: (**a**) ν = 100 mVs^{-1}, (**b**) ν = 200 mVs^{-1}, (**c**) ν = 300 mVs^{-1}.

Table 4.

The electrochemical data for compounds **5a-l**.

Compound	E_{O1} (V)[a]	E_{R1} (V)[b]	$E_{1/2}$ (V)[c]	ΔE (V)
5a	0.684	0.528	0.606	0.156
5b	0.681	0.531	0.606	0.150
5c	0.665	0.549	0.607	0.116
5d	0.665	0.546	0.605	0.119
5e	0.668	0.540	0.604	0.128
5f	0.668	0.537	0.602	0.131
5g	0.690	0.516	0.603	0.174
5h	0.674	0.531	0.602	0.143
5i	0.650	0.531	0.590	0.119
5j	0.656	0.537	0.596	0.119
5k	0.668	0.519	0.593	0.149
5l	0.656	0.534	0.595	0.122

[a] E_{O1}, potentials of anodic peaks O1 vs. Ag/AgCl, at scan rate 0.1 V s^{-1}.
[b] E_{R1}, potentials of cathodic peaks R1 vs. Ag/AgCl, at scan rate 0.1 V s^{-1}.
[c] $E_{1/2}$, half-wave potential of ferrocene's redox couple vs. Ag/AgCl, at scan rate 0.1 V s^{-1}, ($E_{1/2} = (E_{O1}+E_{R1})/2$).

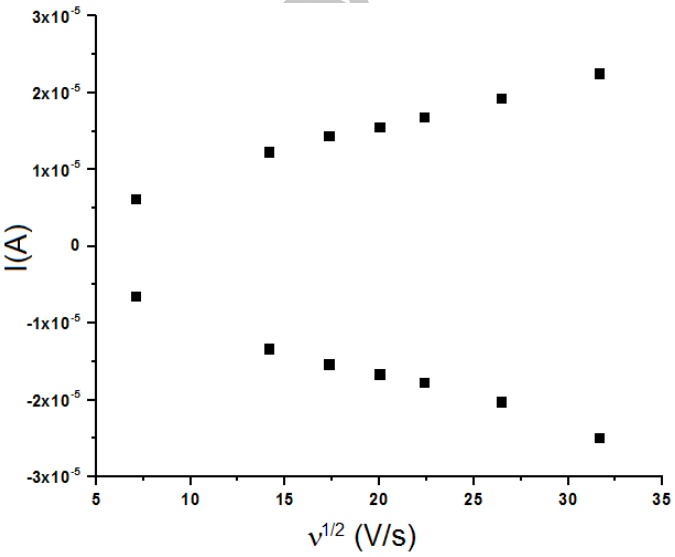

Figure 5. Anodic and cathodic peak currents obtained at different scan rates of 1 mM solution of 2-(3-ferrocenyl-1-phenyl-1-*H*-pyrazol-4-yl)-3-methylthiazolidin-4-one (**5a**) at the glassy carbon electrode in a 0.1 M dichloromethane solution of Bu_4NClO_4.

anodic and cathodic current was not unity and the difference between the oxidation and reduction maxima ($E_p = E_{pa} - E_{pc}$) was 0.135.5 V, which confirms the quasi reversible nature of the system. The electrochemical properties of compounds 5a–l are apparently interesting

and surely deserve additional investigations, but both the extent and the type of the future investigations exceed the scope of this work.

3.5. Antimicrobial activity

The synthesized compounds were screened for antimicrobial activity against a panel of one yeast and four bacterial species. From the results of the microdilution method (Table 5), most of the compounds inhibited examined bacteria and *C. albicans* growth at the highest tested concentration. All synthesized ferrocene derivatives displayed inhibitory activity against the Gram-negative strain *S. enteritidis* at a concentration of 2 mg/mL, while four ferrocene derivatives were unable to inhibit the growth of Gram-negative strain *E. coli* at the same concentration. Except for these four compounds, all studied ferrocene derivatives showed MIC values at a concentration of 2 mg/mL for *E. coli*. Gram-positive strains *E. faecalis* and *S. aureus* were less sensitive against synthesized compounds. MIC values (2 mg/mL) of **5a**, **5f**, **5g**, **5i**, and **5l** were observed for both studied Gram-positive bacteria, while compounds **5c**, **5d**, **5e**, and **5h** were inactive against these bacterial strains, with the MIC values exceeding 2 mg/mL. However, some of the tested compounds (**5a** and **5j**) displayed inhibition at 1 mg/mL against *C. albicans*, suggesting that this yeast is the most sensitive microorganism to the effects of studied ferrocenyl derivatives. The well-known antibiotic ciprofloxacin and antimycotic clotrimazole showed lower MIC values (≤ 20 μg/mL) compared to all synthesized compounds. Generally, according to the obtained results, fungal strain and Gram-negative bacteria seem to be more sensitive to examined compounds than Gram-positive bacterial strains. Similar results for antimicrobial activity were obtained in our previous study with ferrocene containing quinolones [16].

Table 5. Minimal inhibitory concentrations (MIC) of synthesized compounds

Compounds	MIC (mg/mL)				
	E. faecalis	*S. aureus*	*S. enteritidis*	*E. coli*	*C. albicans*
5a	2	2	2	2	1
5b	2	>2	2	2	2
5c	>2	>2	2	2	>2
5d	>2	>2	2	>2	>2
5e	>2	>2	2	2	2
5f	2	2	2	>2	>2
5g	2	2	2	>2	2
5h	>2	>2	2	2	2
5i	2	2	2	>2	2
5j	>2	2	2	2	1
5k	>2	2	2	2	2
5l	2	2	2	2	>2

	MIC (μg/mL)				
Ciprofloxacin	12.5	12.5	<3.125	6.25	-
Clotrimazole	-[a]	-	-	-	20

4. Conclusion

In conclusion, twelve novel 3-ferrocenyl-2-pyrazolyl-1,3-thiazolidin-4-ones were prepared using standard synthetic protocols in moderate to excellent yields (up to 91%). The structures of all the obtained products were determined by the usage of standard spectroscopic methods. Moreover, the proposed structures of products were also confirmed by single-crystal X-ray diffraction analysis that was done for two representative thiazolidin-4-ones (**5k** and **5g**). It was revealed that **5k** and **5g** regardless of significant dissimilarity in the N3-substituent, exhibit very similar structural properties in solid state as formation of dimers and accumulation of ferrocene units in separate sheets. Further, electrochemical investigations, performed by the cyclic voltammetry, showed that all products exhibit reversible one–electron redox couple (attributed to the ferrocene unit) at the similar potential around 200 mV higher than the potential of unsubstituted ferrocene.

The prepared heterocycles were tested against four strains of bacteria (*E. faecalis, S. aureus, S. enteritidis, E. coli*) using microdilution method. It was found that all products show better activity on the Gram-negative than on Gram-positive bacterial strains. Furthermore, antifungal activity of the synthesized ferrocene derivatives tested on the human pathogen yeast *C. albicans* showed that the obtained compounds have more pronounced antifungal potential. Compounds **5a** and **5j** had the highest antimicrobial potential suggesting that this kind of derivatives could serve as a basis for the production of possibly more potent, ferrocene containing antimicrobials.

Supporting Information

X-ray crystalloraphic data in CIF format and copies of ^{1}H NMR and ^{13}C NMR spectra.

Acknowledgement

The authors are grateful to the Ministry of Education, Science and Technological development of the Republic of Serbia for financial support (Grant Nos. 172034 and III43004).

Appendix A. Supplementary data

CCDC 1854965 and 1854966 contains the supplementary crystallographic data for 5k and 5g. These data can be obtained free of charge via http://www.ccdc.cam.ac.uk/conts/retrieving.html, or from the Cambridge Crystallographic Data Centre, 12 Union Road, Cambridge CB2 1EZ, UK; fax: (+44) 1223-336-033; or e-mail: deposit@ccdc.cam.ac.uk.

Supplementary data to this article (Figures S1 and S2) can be found online.

References

[1] P. M. Hawkey. *J. Antimicrob. Chemother*. 62 (2008) 1–19.

[2] R. Cantón. *Clin. Microbiol. Infect*. 15 (2009) 20–25.

[3] N. Metzler-Nolte, U. Schatzschneider. Bioinorganic chemistry: a practical course , Walter de Gruyter GmbH & Co KG, Berlin, 1990, pp. 120–123.

[4] I. Apostolidis, K. Liaras, A. Geronikaki, D. Hadjipavlou-Litina, A. Gavalas, M. Soković, J. Glamočlija, A. Ćirić. *Bioorg. Med. Chem*. 21 (2013) 532–539.

[5] D. Havrylyuk, B. Zimenkovsky, O. Vasylenko, L. Zaprutko, A. Gzella, R. Lesyk. *Eur. J. Med. Chem*. 44 (2009) 1396–1404.

[6] M. Sarkis, D. N. Tran, M. C. D. Lang, C. Garbay, E. Braud. *Synlett* 25 (2014) 1257–1262.

[7] D. Kaminskyy, D. Khyluk, O. Vasylenko, R. Lesyk. *Tetrahedron lett*. 53 (2012) 557–559.

[8] C. Bathula, S. Tripathi, R. Srinivasan, K. K. Jha, A. Ganguli, G. Chakrabarti, S. Singh, P. Munshi, S. Sen. *Org. Biomol. Chem*. 14 (2016) 8053–8063.

[9] C. N. Ambeu, C. D. Dago, W. K. Coulibaly, Y. A. Békro, J. A. Mamyrbekova-Békro, B. Foll-Josselin, A. Defontaine, C. Delehouzé, S. Bach, S. Ruchaud, R. L. Guével, A. Corlu, P. Jéhan, F. Lambert, N. L. Yondre, J. P. Bazureau. *Med. Chem. Res*. 25 (2016) 2940–2958.

[10] A. Geronikaki, E. Babaev, J. Dearden, W. Dehaen, D. Filimonov, I. Galaeva, V. Krajneva, A. Lagunin, F. Macaev, G. Molodavkin, V. Poroikov, S. Pogrebnoi, V. Saloutin, A. Stepanchikova, E. Stingaci, N. Tkach, L. Vladg, T. Voronina. *Bioorg. Med. Chem. 12* (2004) 6559–6568.

[11] R. E. Sammelson, P. Caboni, K. A. Durkin, J. E. Casida. *Bioorg. Med. Chem.* 12 (2004) 3345–3355.

[12] J. S. Kumar, J. Prabhakaran, V. Arango, R. V. Parsey, M. D. Underwood, N. R. Simpson, S. A. Kassir, V. J. Majo, R. L. Van Heertum, J. J. Mann. *Bioorg. Med. Chem. Lett.* 14 (2004) 2393–2396.

[13] A. Bekhit, T. Abdel-Aziem. *Bioorg. Med. Chem.* 12 (2004) 1935–1945.

[14] P. Baraldi, I. Beria, P. Cozzi, N. Bianchi, R. Gambari, R. Romagnoli. *Bioorg. Med. Chem.* 11 (2003) 965–975.

[15] rM. Joksović, Z. Ratković, M. Vukićević, R. D. Vukićević. *Synlett* 16 (2006) 2581–2584.

[16] A. Pejović, I. Damljanović, D. Stevanović, A. Minić, J. Jovanović, V. Mihailović, J. Katanić, G. A. Bogdanović. *J. Organomet. Chem*. 846 (2017) 6–17.

[17] A. Pejović, B. Danneels, T. Desmet, B. T. Cham, T. V. Nguyen, N. Radulović, R. D. Vukićević, M. D'hooghe. *Synlett* 26 (2015) 1195–1200.

[18] A. Pejović, I. Damljanović, D. Stevanović, M. Vukićević, S. B. Novaković, G. A. Bogdanović, N. Radulović, R. D. Vukićević. *Polyhedron* 31 (2012) 789–795.

[19] A. Pejović, M. S. Denić, D. Stevanović, I. Damljanović, M. Vukićević, K. Kostova, M. Tavlinova-Kirilova, P. Randjelović, N. M. Stojanović, G. A. Bogdanović, P. Blagojević, M. D'hooghe, N. S. Radulović, R. D. Vukićević. *Eur. J. Med. Chem*. 83 (2014) 57–73.

[20] Agilent, CrysAlis PRO, Agilent Technologies, Yarnton, Oxfordshire, England, 2013.

[21] G. M. Sheldrick, *Acta Crystallogr*., Sect. A 64 (2008) 112.

[22] C. F. Macrae, P. R. Edgington, P. Mc Cabe, E. Pidcock, G. P. Shields, R. Taylor, M. Towler, J. van de Streek, *J. Appl. Crystallogr*. 39 (2006) 453.

[23] L.J. Farrugia, J. Appl. Crystallogr. 32 (1999) 837.

[24] A. L. Spek, J. Appl. Crystallogr. 36 (2003) 7.

[25] M. Nardelli, J. Appl. Crystallogr. 28 (1995) 659.

[26] S. D. Sarker, L. Nahar, Y. Kumarasamy. *Methods* 42 (2007) 321–324.

[27] CLSI. *Methods for Dilution Antimicrobial Susceptibility Tests for Bacteria That Grow Aerobically*; Approved Standard—Ninth Edition. CLSI document M07–A9. Wayne, PA: Clinical and Laboratory Standards Institute; 2012.

[28] NCCLS. *Reference Method for Broth Dilution Antifungal Susceptibility Testing of Filamentous Fungi; Approved Standard.* NCCLS document M38–A [ISBN 1–56238–470–8]. NCCLS, 940 West Valley Road, Suite 1400, Wayne, Pennsylvania 19087–1898 USA, 2002a.

[29] NCCLS. *Reference Method for Broth Dilution Antifungal Susceptibility Testing of Yeasts; Approved Standard—Second Edition.* NCCLS document M27-A2 [ISBN 1–56238–469–4]. NCCLS, 940 West Valley Road, Suite 1400, Wayne, Pennsylvania 19087–1898 USA, 2002b.

[30] R. K. Rawal, R. Tripathi, S. Kulkarni, R. Paranjape, S. B. Katti, C. Pannecouque, E. De Clercq. *Chem. Biol. Drug. Des*. 72 (2008) 147–154.

[31] R. K. Rawal, T. Srivastava, W. Haq, S. B. Katti. *J. Chem. Res*. 5 (2004) 368–369.

[32] T. Srivastava, W. Haq, S. B. Katti. *Tetrahedron* 58 (2002) 7619–7624.

[33] J. Safaei-Ghomi, M. Navvab, H. Shahbazi-Alavi, *Ultrason. Sonochem.* 31 (2016) 102–106.

[34] Z. R. Ratković, Z. D. Juranić, T. P. Stanojković, D. D. Manojlović, R. D. Vukićević, N. S. Radulović, M. D. Joksović. *Bioorg. Chem.* 38 (2010) 26–32.

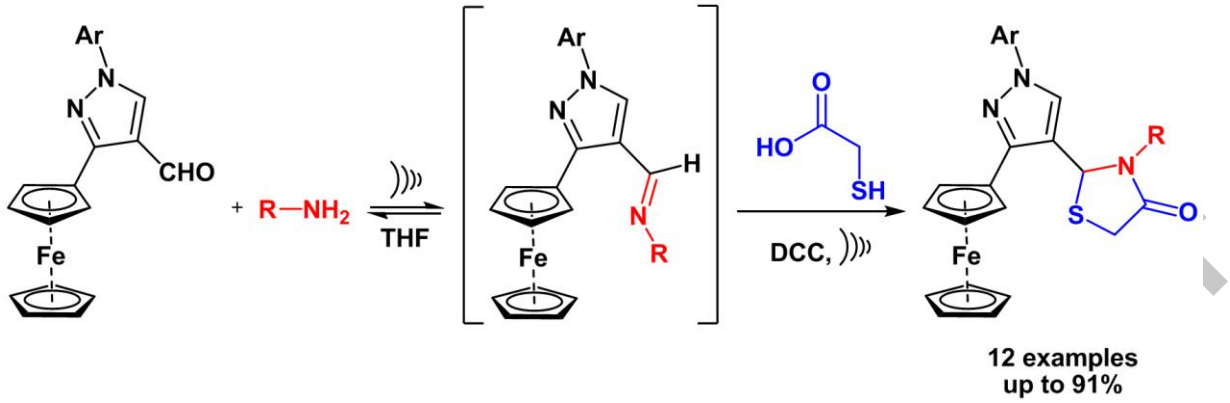

The preparation of a new series of 3-ferrocenyl-2-pyrazolyl-1,3-thiazolidin-4-ones by standard synthetic protocol is described.

Twelve newly synthesized compounds were full spectrally and electrochemically characterized. The structures of two compounds were corroborated by X-ray single-crystal analysis. Antimicrobial activity of all synthesized compounds were evaluated.